

Charge carrier concentration and mobility in alkali silicates

Jean-Louis Souquet,¹ Marcio Luis Ferreira Nascimento,^{2,a),b)} and Ana Candida Martins Rodrigues^{3,a),c)}

¹Laboratoire d'Electrochimie et de Physicochimie des Matériaux et des Interfaces, ENSEEG, BP 75, Saint Martin D'Hères Cedex 38402, France

²Vitreous Materials Laboratory, Institute of Humanities, Arts and Sciences, Federal University of Bahia, Rua Barão de Jeremoabo s/n, PAF 3, Ondina University Campus, Salvador-BA 40170-115, Brazil

³Departamento de Engenharia de Materiais, Laboratório de Materiais Vítreos, Universidade Federal de São Carlos, São Carlos-SP 13565-905, Brazil

(Received 24 July 2009; accepted 11 November 2009; published online 21 January 2010)

The respective contributions of the charge carrier concentration and mobility to the ionic conductivity in glasses remain an open question. In the present work we calculate these two parameters from conductivity data as a function of temperature below and above the glass transition temperature, T_g . The basic hypothesis assumes that ionic displacement results from the migration of cationic pairs formed by a partial dissociation, which is a temperature-activated process. Below T_g their migration would follow a temperature-activated mechanism, while a free volume mechanism prevails above this temperature, leading to a deviation from the Arrhenius behavior. Expressions are formulated for the variation in ionic conductivity as a function of temperature in the supercooled and glassy states. Fitting the experimental data with the proposed expressions allows for the determination of characteristic parameters such as the charge carrier formation and migration enthalpies. Based on these values, it is then possible to calculate the charge carrier concentration and mobility in the entire temperature range. At room temperature, the mobility of effective charge carriers is estimated close to $10^{-4} \text{ cm}^2 \text{ s}^{-1} \text{ V}^{-1}$ for alkali disilicates glasses under study, while the ratio between the number of effective charge carriers and the total number of alkali cations is estimated to be from 10^{-8} to 10^{-10} , comparable to the concentration of intrinsic defects in an ionic crystal or dissociated species from a weak electrolyte solution. © 2010 American Institute of Physics. [doi:10.1063/1.3271154]

I. INTRODUCTION

In a material whose electrical conduction results from the migration of a unique charge carrier species, i.e., either electron or ion, the electrical conductivity, σ , is expressed as $\sigma = n_e e \mu$, where n_e is the effective charge carrier concentration, e is the charge for the single charge species, and μ is its electrical mobility.

In the case of ion conductive glasses, the absence of experimental data on n_e or μ leads to different interpretations, assuming that either all the ions move simultaneously with a low mobility, or only a small fraction of them move with a higher mobility at any given time. In other words, glasses are considered as either strong¹ or weak electrolytes.² The individual determination of charge carrier concentration and mobility is thus of crucial importance for a better understanding of conductivity mechanisms.

The charge carrier concentration and mobility of most electronic conductors such as semiconductors can be determined separately by measuring both Hall's coefficient and the conductivity.³ However, in ionic conductors, the mobility

of ions is lower than that of electrons in a semiconductor by about five orders of magnitude, and the ionic Hall voltage is expected to be in the microvolt to nanovolt range. Its detection is considerably hindered by the existence of a comparatively huge offset voltage between the Hall electrodes. The so-called "continuous" methods using dc currents and uniform magnetic fields are no longer operative. More sophisticated ac techniques have thus been employed to determine ionic mobility in highly silver conductive crystals^{4,5} and glasses.⁶

Another technique, which derives from the characterization of MOS (metal-oxide-silicon) devices and is known as C-V (capacitance-voltage) measurement, has been proposed to determine the charge carrier concentration in silica glasses with low alkali content (10^{-2} – 10 ppm).^{7,8} At higher sodium contents, the charge carrier concentration has been deduced from space charge capacitance measurements as a function of the bias voltage applied between two blocking electrodes.⁹

In this paper, we propose a method to separate the contribution of charge carrier concentration from that of mobility, based on conductivity data above and below the glass transition temperature, T_g . Basically, we assume that charge carriers are formed by a thermally activated dissociation process. Their migration is assumed to also follow an activated mechanism below T_g , but a free volume mechanism prevails above this temperature. As previously shown,¹⁰ fitting the

^{a)} Authors to whom correspondence should be addressed.

^{b)} <http://www.lamav.ufba.br>. Also at PROTEC, PEI — Postgraduate Program in Industrial Engineering, Polytechnic School, Federal University of Bahia, Rua Aristides Novis 2, Federação, 40210-630 Salvador-BA, Brazil. Electronic mail: mlfn@ufba.br.

^{c)} Electronic mail: acmr@ufscar.br.

experimental data with this model enables one to determine characteristic parameters such as the charge carrier formation and migration enthalpies, which then allows the charge carrier concentration and mobility to be calculated. We applied this procedure to lithium, sodium, and potassium disilicate glasses ($M_2O \cdot 2SiO_2$, $M=Li,Na,K$), for which electrical conductivity data are available below and above T_g .

II. IONIC CONDUCTIVITY IN MOLTEN AND GLASSY ALKALI DISILICATES

A. Dependence of ion transport on temperature, a microscopic approach

1. Below the glass transition temperature

Ionic conductivity, σ , in molten or glassy silicates results from alkali migration in the silicate network. Conductivity data are available in a large range of temperatures below and above the glass transition temperature. Below T_g , σ , or σT follows a temperature-activated mechanism and is well represented by an Arrhenius law,

$$\sigma T = A \exp(-E_A/k_B T), \quad (1)$$

where E_A is the activation energy, A is the pre-exponential term, while T and k_B have their usual meaning.

This Arrhenius behavior can be justified by a classical approach initially developed for ionic crystals and then extended to ionic conductive glasses.¹¹ From a microscopic point of view, it has been proposed that alkali transport occurs by interstitial cationic pairs, formed by two alkali cations sharing the same negatively charged nonbridging oxygen, ^{12,13} which is an entity equivalent to a Frenkel defect if we refer to an ionic crystal, or to a dissociated cation if we refer to electrolytic solutions. Since the relative dielectric constant, ϵ , of inorganic alkali disilicate glasses is low ($5 < \epsilon < 9$), ionic species must be strongly associated. For instance, most monovalent cations will each be associated with a nonbridging oxygen atom. Such an associated cation may be regarded as being in a normal position, hence defining a regular cationic site. On the other hand, the formation of interstitial cationic pairs would result from the dissociation of an alkali cation from its normal site, allowing it to jump to a neighboring cationic site that is already occupied, as shown in Fig. 1(a). Since the required energy to escape from a normal position is expected to be much higher than the mean thermal energy, $k_B T$, the concentration of such positively charged defects, n_+ , is very low compared to the total concentration of alkali cations, n . In other words, glasses can be considered *weak* electrolytes.

In that case, the chemical equilibrium between alkali cations in regular sites and in interstitial positions leads to the following relationship:

$$n_+ = n \exp\left(-\frac{\Delta G_f}{2k_B T}\right), \quad (2)$$

where $\Delta G_f = \Delta H_f - T\Delta S_f$ is the free energy associated with the simultaneous formation of an interstitial pair and a cationic “vacancy.” ΔH_f and ΔS_f are their formation enthalpy and entropy, respectively.

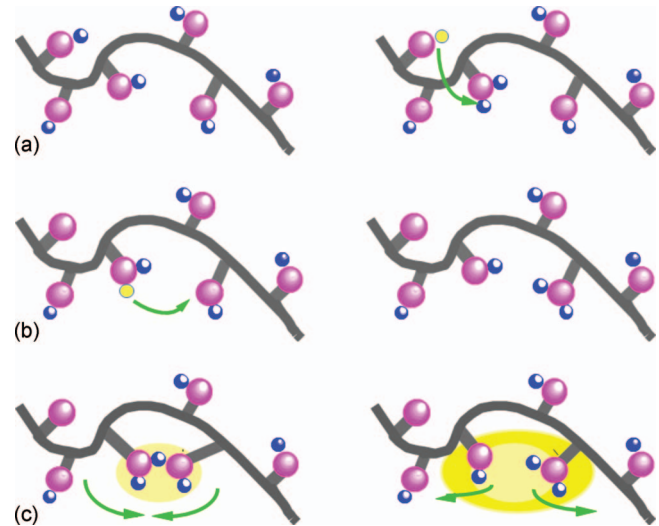


FIG. 1. Schematic representation of conduction mechanisms below and above T_g (after Ref. 17). (a) Below and above T_g : representation of the formation of an interstitial pair, (ΔG_f). (b) Below T_g : interstitial pair migration following an activated mechanism, (ΔG_m). (c) Above T_g : interstitial pair migration by a free volume mechanism involving cooperative chain movement.

This positively charged interstitial cationic pair could then migrate from one interstitial position to another when an electric field is applied [Fig. 1(b)]. A Haven ratio between 0.3 and 0.6, which is usually found for oxide glasses,¹⁴ suggests that ionic transport is expected to occur by the migration of such a cationic pair from one nonbridging oxygen to another rather than by a simple vacancy mechanism. This displacement is characterized by a mobility μ_+ . Using the Nernst–Einstein relation, this mobility can be expressed as a function of the diffusion coefficient D_σ of the charge carriers and then as a function of their characteristic attempt frequency ν and jump distance, λ ,

$$\mu_+ = \frac{eD_\sigma}{k_B T} = \frac{e\lambda^2\nu}{6k_B T}\Omega, \quad (3)$$

where Ω is the probability of a successful jump. In case of a thermally activated mechanism, $\Omega = \Omega_1$ is a function of the required free energy for migration ΔG_m ,

$$\Omega = \Omega_1 = \exp\left(-\frac{\Delta G_m}{k_B T}\right). \quad (4)$$

Finally, the following expression for the cationic conductivity can be then proposed:

$$\sigma = en_+\mu_+ = n \frac{e^2\lambda^2\nu}{6k_B T} \exp\left(-\frac{\Delta G_f/2 + \Delta G_m}{k_B T}\right), \quad (5)$$

or, after separation of the enthalpic and entropic terms,

$$\sigma = n \frac{e^2\lambda^2\nu}{6k_B T} \exp\left(\frac{\Delta S_f/2 + \Delta S_m}{k_B}\right) \exp\left(-\frac{\Delta H_f/2 + \Delta H_m}{k_B T}\right). \quad (6)$$

Formally, the pre-exponential term in Eq. (6) is temperature dependent, justifying the representation of experimental data by $\log_{10} \sigma T$ as a function of reciprocal temperature. This relationship reduces to the experimentally observed Arrhen-

ius law [Eq. (1)] by identification of the experimental value of E_A as

$$E_A = \Delta H_f/2 + \Delta H_m, \quad (7)$$

and the pre-exponential term A as

$$A = n \frac{e^2 \lambda^2 \nu}{6k_B} \exp\left(\frac{\Delta S_f/2 + \Delta S_m}{k_B}\right). \quad (8)$$

Experimental values for E_A and A can be deduced easily from the linear curves obtained in an Arrhenius plot of σT . For silicates, typical experimental values for A are between 10^4 and 10^5 K·S/cm and for E_A between 0.5 and 1 eV. The pre-exponential term $ne^2\lambda^2\nu/6k_B$ can be assessed numerically using $n=10^{22}$ ions/cm³, $\lambda=\sqrt[3]{1/n}$, and $\nu=10^{13}$ Hz, yielding $A \approx 10^5$ K·S/cm, which is close to typical experimental values. The implication of this result is that the entropic terms in the exponential [Eq. (8)] are very low compared to k_B , and consequently, the free energies ΔG_f and ΔG_m reduce to the enthalpies ΔH_f and ΔH_m . Equation (2) may thus be rewritten as

$$n_+ = n \exp\left(-\frac{\Delta H_f}{2k_B T}\right). \quad (9)$$

2. Above the glass transition temperature

Above the glass transition temperature, T_g , the experimental ionic conductivity in the supercooled liquid increases over values extrapolated from the Arrhenius behavior below T_g . This increase is interpreted as resulting from the occurrence of a different migration mechanism in addition to the activated migration mechanism previously described. This high temperature process, schematically represented in Fig. 1(c), is associated with a free volume mechanism¹⁵ involving the local movement of the silicate chains.

This free volume mechanism, which has been theoretically justified by Cohen and Turnbull¹⁶ for cooperative molecular transport that controls viscous flow in liquids and glasses, assumes that a moving species can escape from a cage formed by its nearest neighbors when the random density fluctuations produce an adjoining cage large enough to allow for a jump from one cage to another. These fluctuations can be described by an exchange of the so-called “free” volume, i.e., without enthalpic cost, between the two neighboring cages. Thus, the corresponding displacement probability, Ω_2 , may be written as an exponential function of the ratio between the smallest free volume V_f^* required for a jump and the available mean volume \bar{V}_f .

$$\Omega_2 = \exp(-V_f^*/\bar{V}_f) \quad (10)$$

The value of the mean available free volume is usually approximated by

$$\bar{V}_f = V_0(\alpha_l - \alpha_g)(T - T_0), \quad (11)$$

where α_l and α_g are the thermal expansion coefficients of the liquid and the corresponding glass, and V_0 is the volume of the moving species extrapolated at T_0 , the ideal glass transition temperature at which the free volume disappears. In the liquid state, in addition to the anharmonic thermal vibrations,

an increasing number of voids contribute to the thermal expansion. In this approach, the difference $\alpha_l - \alpha_g$ thus represents the volume expansion due to this increase in the number of voids in the liquid. At T_0 the free volume tends towards zero, since the structural relaxation time tends towards infinity. Thus, below this temperature, the silicate chains no longer cooperate with the migration process. This ideal glass transition temperature lies below the experimental glass transition temperature, T_g , which may be determined, for instance, by DSC or dilatometry. A semiempirical rule,¹⁷ $T_0 = (3/4)T_g$, allows one to estimate the ideal glass temperature when T_g is known.

In this case, and according to the present model, the moving species is an interstitial pair transferred from one nonbridging oxygen site to another, allowing charge transfer along a silicate chain. Above T_0 , the charge transfer may occur by either an activated jump (Ω_1) or a free volume mechanism (Ω_2), and the total jump probability Ω is given by

$$\Omega = \Omega_1 + \Omega_2(1 - \Omega_1), \quad (12)$$

which suggests that the second (free volume) process, Ω_2 , only applies to the unsuccessful first (activated) process, Ω_1 . Under such conditions and according to Eq. (9), the cationic conductivity becomes

$$\sigma T = n \frac{e^2 \lambda^2 \nu}{6k_B} \exp\left(-\frac{\Delta G_f/2}{k_B T}\right) [\Omega_1 + \Omega_2(1 - \Omega_1)]. \quad (13)$$

At temperatures above T_g , Ω_2 is expected to prevail over Ω_1 (Ref. 10) and Eq. (13) becomes

$$\sigma T = n \frac{e^2 \lambda^2 \nu}{6k_B} \exp\left(-\frac{\Delta G_f/2}{k_B T}\right) \exp\left(-\frac{V_f^*}{\bar{V}_f}\right). \quad (14)$$

Expressing the V_f^*/\bar{V}_f ratio as a function of V_0 and the ideal glass transition temperature T_0 [according to Eq. (11)], one has

$$\sigma T = A \exp\left(-\frac{E_A^*}{k_B T}\right) \exp\left[-\frac{B}{k_B(T - T_0)}\right], \quad (15)$$

with $E_A^* = \Delta H_f/2$ being the activation enthalpy and $B/k_B = V_f^*/V_0(\alpha_l - \alpha_g)$.

Equation (15) is formally the same equation proposed by Dienes¹⁸ and later by Macedo and Litovitz¹⁹ to describe the variation of viscosity with temperature. For this reason, we will call it the DML equation. This equation has previously been found to accurately describe conductivity data of molten silicates and salt-polymer complexes in the supercooled liquid state.^{10,20–22} From Eqs. (15) and (7) it can be seen that the activation energy $E_A^* = \Delta H_f/2$ in the DML equation is different from the activation energy $E_A = \Delta H_f/2 + \Delta H_m$ below T_g . Accordingly, the determination of E_A and E_A^* from experimental data below and above T_g allows us to calculate both ΔH_f and ΔH_m .

Note that the free volume model chosen to describe the charge carrier migration implies a cooperative displacement of neighboring atoms or chain segments as represented in

Fig. 1(c). This cooperative displacement could also be described by an entropic model as proposed by Adam and Gibbs.²³

Following this model, this cooperative rearrangement depends on the supercooled liquid configurational entropy, S_c . According to Kauzmann²⁴ this configurational entropy decreases with temperature and disappears at a temperature T_K at which the entropy of the overcooled liquid would be the same than that of the crystal from the same composition.

Applying this model to express the probability of a cooperative displacement (Ω_2) to take place leads to $\Omega_2 = \exp(-C/TS_c)$, where C is a constant, proportional to a critical configurational entropy, s_c^* , and to the free energy barrier, $\Delta\mu$, which hinders the cooperative rearrangement per chain segment. The supercooled liquid configurational entropy is $S_c = \int_{T_K}^T (\Delta C_p/T)DT$, where ΔC_p is the difference between the heat capacity of the liquid and the crystal. Since ΔC_p can be approximated by $\Delta C_p \approx D/T$ (D is a constant),²⁵ thus, S_c as a function of temperature T may be written as $S_c = D(T - T_K)/TT_K$. This approach leads finally to a formally analogous expression as Eq. (15), but with different interpretation for the parameters B and T_0 . In this entropic model, $B = s_c^* \cdot \Delta\mu T_K / D$ and the ideal glass transition temperature T_0 at which the free volume, as defined by Cohen and Turnbull, disappears is identified to the Kauzmann temperature T_K .

III. EXPERIMENTAL CONDUCTIVITY DATA AND DETERMINATION OF CHARGE CARRIER FORMATION AND MIGRATION ENTHALPIES

In order to cover a broad range of temperatures and minimize discrepancies, electrical conductivity data were taken from various authors.^{26–47} The design of conductivity cells is obviously different below and above the glass transition temperature. Below T_g , glass samples are generally discs of 1–3 cm diameter and 1–5 mm thickness. Depending on the authors, platinum, gold, or silver electrodes are deposited by sputtering, vacuum evaporation, or painted onto the two circular faces. Electrical measurements are taken using dc techniques or impedance spectroscopy in the case of more recent data. For conductivity values lower than 10^{-3} S/cm and an applied voltage below 200 mV, the electrode polarization is low and no significant differences can be detected between the two techniques. At higher temperatures, over T_g , the molten silicates are contained in platinum crucibles and two platinum electrodes are immersed in the melt. The cell is precalibrated at room temperature with a KCl solution. To prevent electrode polarization, the melt resistance is determined in a frequency range in which the resistance is not frequency dependent, generally around 10 kHz.

For the purpose of this work a total of 124 experimental conductivity data from Refs. 26–47 have been collected. However, for clarity, only selected conductivity data for lithium, sodium, and potassium disilicates are presented in Arrhenius coordinates in Fig. 2. The corresponding number N of data collected for each composition in the glassy or supercooled liquid range is specified on Tables I and II.

Conductivity data above T_g were fitted using the DML Eq. (15), which *a priori* contains four adjustable parameters, A , B , T_0 , and E_A^* . In general, when fitting experimental data

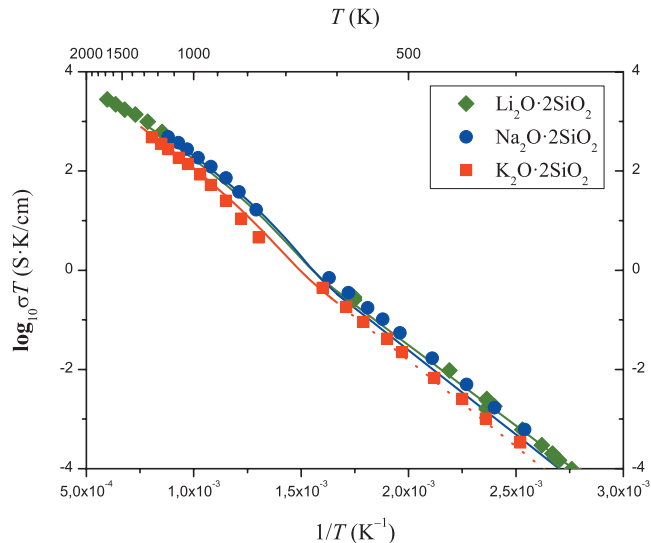


FIG. 2. σT as a function of temperature in Arrhenius coordinates. For clarity, only selected data are represented for lithium (\blacklozenge), sodium (\bullet), and potassium (\blacksquare) disilicate glasses. For lithium disilicate data of Bockris (Ref. 26) over T_g , and from Dale *et al.* (Ref. 27), Hahnert *et al.* (Ref. 28), Higby and Shelby (Ref. 29), Kone *et al.* (Ref. 30), Leko (Ref. 32), Mazurin and Borisovskii (Ref. 33), Mazurin and Tsekhomskii (Ref. 34), Souquet *et al.* (Ref. 36), and Yoshiyagawa and Tomozawa (Ref. 38), below T_g . All data for sodium and potassium disilicates are from Caillot *et al.* (Ref. 10). Full lines represent the best fit of our model with all data from Refs. 26–47.

with such a number of adjustable parameters, it is always possible to obtain a good fit. This is especially valid in the case of Eq. (15), which contains the product of two temperature-dependent exponentials and successive fits may lead to different sets of adjustable parameters. We then restricted the number of adjustable parameters by fixing the ideal glass transition temperature T_0 and the pre-exponential term A , and determined the two remaining ones, B and E_A^* . Parameter A was extrapolated from the Arrhenius plots of conductivity data below T_g , while T_0 was estimated from T_g by $T_0 = (3/4)T_g$.¹⁷ Fixed and calculated parameters are reported in Table I. As can be seen, the resulting values of A remain very close to 10^5 K·S/cm, as estimated previously. Note that the dispersion of experimental data leads to a mathematical error in A , which is negligible on a log scale.

All the calculations were performed using Levenberg–Marquardt nonlinear fitting and ORIGIN™ software. To improve the accuracy of the numerical calculation for each composition, we used a number of experimental values N between 14 and 27, which were below and above the glass transition temperature. The number of experimental data points N and respective χ^2 results for each composition are listed in Table I.

Below T_g , the activation energy E_A is calculated from the Arrhenius representation of experimental data. Since $E_A = \Delta H_f/2 + \Delta H_m$ and $E_A^* = \Delta H_f/2$, the migration enthalpy is simply $\Delta H_m = E_A - E_A^*$. Table II lists the corresponding values.

IV. DISCUSSION

A. Critical free volume for ionic transport above the glass transition temperature

The B parameter for conductivity in all the systems is conventionally expressed in eV, as shown in Table I, despite

TABLE I. Numerical values for E_A^* and B (in eV) determined by the best fit of experimental data over the glass transition temperature with the DML Eq. (15). The corresponding number of experimental data points N and χ^2 values are also indicated. The mathematical accuracy is $\pm 10^{-2}$ and 3×10^{-3} eV for E_A^* and B , respectively. Values of the pre-exponential term, A , and T_0 ($T_0 = 3/4T_m$) are also reported.

	A (K S/cm)	T_0 (K)	E_A^* (eV)	B (eV)	N	χ^2 (%)
$\text{Li}_2\text{O} \cdot 2\text{SiO}_2$	$(1.1 \pm 1.4) \times 10^5$	545	0.48	0.042	22	0.4
$\text{Na}_2\text{O} \cdot 2\text{SiO}_2$	$(2.1 \pm 2.3) \times 10^5$	551	0.51	0.033	27	0.5
$\text{K}_2\text{O} \cdot 2\text{SiO}_2$	$(1.7 \pm 1.5) \times 10^5$	568	0.55	0.038	14	0.04

the fact that the aforementioned microscopic model of Cohen and Turnbull¹⁶ implies that no energy is involved in the free volume mechanism. According to the free volume model, the B parameter depends on the ratio of the critical free volume V_f^* and V_0 , the extrapolated volume at T_0 of the moving species in the supercooled liquid. B and the V_f^*/V_0 ratio are related according to the equation $B/k_B = V_f^*/V_0(\alpha_l - \alpha_g)$, where α_l and α_g are the volumetric thermal expansion of the liquid and corresponding glass.

Table III lists the values for α_l and α_g collected for the three alkali disilicates under study and their calculated ratios $V_f^*/V_0 = B(\alpha_l - \alpha_g)/k_B$. The V_f^*/V_0 ratios are around 10^{-2} . These values come from the low values of the B parameters $\sim 3 \times 10^{-2}$ eV (Table I), and are in agreement. Such low values, between 10^{-2} and 10^{-1} eV, are also found for ionic transport in salt-polymer complexes¹⁷ when conductivity data are fitted by a Vogel–Fulcher–Tammann–Hesse equation.

The low values of V_f^*/V_0 ratio and B may be interpreted qualitatively by the fact that the charge transfer along the macromolecular chains requires a relatively low amount of free volume, lower than that for a cationic pair associated to a nonbridging oxygen. As suggested in Fig. 1, if the charge transfer occurs by an interstitial pair mechanism, the alkali cations need only a limited displacement between two neighboring nonbridging oxygens to transfer a positive charge.

B. An estimation of charge carrier concentration and mobility in alkali silicates below the glass transition temperature

Table II compares the enthalpies for charge carrier formation and migration deduced from the experimental values of activation energies E_A and E_A^* . The values for the charge carrier migration do not vary significantly with the type of alkali cation. In the three compositions investigated, the charge carrier formation requires an enthalpy of about 1 eV, and their migration enthalpy a value close to 0.15 eV.

TABLE II. Characteristic parameters, E_A , ΔH_f , and ΔH_m , for ionic conductivity below the glass transition temperature. The mathematical accuracy does not exceed 2×10^{-2} eV at these values. The number of experimental data points N and respective χ^2 values are also reported.

	E_A (eV)	ΔH_f (eV)	ΔH_m (eV)	N	χ^2 (%)
$\text{Li}_2\text{O} \cdot 2\text{SiO}_2$	0.65	0.96	0.17	25	1.5
$\text{Na}_2\text{O} \cdot 2\text{SiO}_2$	0.68	1.02	0.17	21	13
$\text{K}_2\text{O} \cdot 2\text{SiO}_2$	0.70	1.10	0.15	15	0.7

Using these calculated values, it is then possible to estimate the relative concentration n_+/n of charge carriers in the glassy state using the Eq. (9), taking n from density data as 2.8×10^{22} at. cm^{-3} for $\text{Li}_2\text{O} \cdot 2\text{SiO}_2$ (LS_2), 2.5×10^{22} at. cm^{-3} for $\text{Na}_2\text{O} \cdot 2\text{SiO}_2$ (NS_2), and 2.1×10^{22} at. cm^{-3} for $\text{K}_2\text{O} \cdot 2\text{SiO}_2$ (KS_2). The mobility μ_+ is then calculated from the relationship $\mu_+ = \sigma/en_+$. The calculated temperature dependence of the relative concentration in charge carriers and their mobility are represented in Figs. 3 and 4.

As Fig. 4 indicates, mobility values at room temperature are between 10^{-3} and 10^{-4} $\text{cm}^2 \text{s}^{-1} \text{V}^{-1}$. It is interesting to note that similar mobility values, measured by Hall effect, are found for silver in crystalline^{4,5,50} or glassy⁶ silver-conducting electrolytes. The restrictive choice of silver solid electrolytes investigated via Hall effect measurements is due to the fact that these materials are the highest conductive solid electrolytes at room temperature, allowing for high Hall voltages. From Fig. 4 higher mobility for the larger cations may be observed. This result comes from a slow decrease in the values of ΔH_m with increasing ionic radius (Table II). Note that these differences are in the limit of the mathematical accuracy mentioned on the Table II caption. Nevertheless, should this result be confirmed for other comparable alkali content, it could be interpreted by the fact that the interstitial pairs formed with the larger cations would be, for steric reasons, less deeply trapped in the nonbridging oxygen Coulombic wall.

In $\text{C}_5\text{H}_6\text{NAg}_5\text{I}_6$ at 20 °C, Newman *et al.*⁵⁰ obtained a Ag^+ ion mobility of $3.7 \text{ cm}^2 \text{ s}^{-1} \text{ V}^{-1}$ by extracting Hall voltages from 10 to 100 nV with an applied magnetic field of 0.1–1 T. Using ac Hall techniques on $x\text{AgI} \cdot (1-x)\text{AgPO}_3$ glasses ($0 < x < 0.5$), Clement *et al.*⁶ found a Ag^+ mobility value of $(6 \pm 2) \times 10^{-4} \text{ cm}^2 \text{ s}^{-1} \text{ V}^{-1}$ at 25 °C independent of x . Also measuring at room temperature, Funke and

TABLE III. Calculated volume ratios V_f^*/V_0 required for the migration process above the glass transition temperature, and experimental values of volumetric thermal expansion coefficient in the liquid (α_l) and glassy (α_g) states.

	α_l ($\times 10^{-7}/\text{K}$)	α_g ($\times 10^{-7}/\text{K}$)	Reference	V_f^*/V_0
$\text{Li}_2\text{O}\cdot 2\text{SiO}_2$	373	360	48	0.036
$\text{Na}_2\text{O}\cdot 2\text{SiO}_2$	1395	495	49	0.033
$\text{K}_2\text{O}\cdot 2\text{SiO}_2$	1455 ^a	558	49	0.039

^a α_l of potassium disilicate is calculated from density data.

Hackenberg⁴ found a Ag^+ mobility close to $10^{-4} \text{ cm}^2 \text{ s}^{-1} \text{ V}^{-1}$ for $\alpha\text{-AgI}$ and Stuhmann *et al.*⁵ found the same mobility for $\alpha\text{-RbAg}_4\text{I}_5$.

From these data and the values calculated in the present work, it is interesting to observe that, regardless of the solid electrolyte and the nature of the charge carrier, the room temperature ionic mobility values are of the same order of magnitude close to $10^{-4} \text{ cm}^2 \text{ s}^{-1} \text{ V}^{-1}$. Obviously, these values are seven orders of magnitude lower than the mobility of electrons or holes in a semiconductor,³ but, interestingly, they are of the same order of magnitude as that of the ionic mobility extrapolated to infinite dilution in aqueous solutions.⁵¹

A consequence of these results is that the differences in conductivity values result mainly from the number of effective charge carriers. In fact, considering experimental electrical conductivity and mobility in crystalline fast ionic conductors $\alpha\text{-AgI}$ (Ref. 4) and $\alpha\text{-RbAg}_4\text{I}_5$,⁶ it can be seen that all silver ions are effective charge carriers. In $\text{C}_5\text{H}_6\text{NAg}_5\text{I}_6$, $5 \times 10^{-2} \text{ Ag}^+$ cations would be simultaneously mobile,⁵⁰ while in the silver phosphate glasses AgPO_3 , the fraction of mobile silver cations is only 3×10^{-7} .⁵ The latter value is comparable to the concentration of intrinsic defects in a crystalline structure,⁵² or to that of dissociated species in a weak electrolyte.⁵¹

In the present study on alkali disilicates, the calculated concentration of effective charge carriers at room temperature would be lower, i.e., only a fraction of 10^{-8} to 10^{-10} of

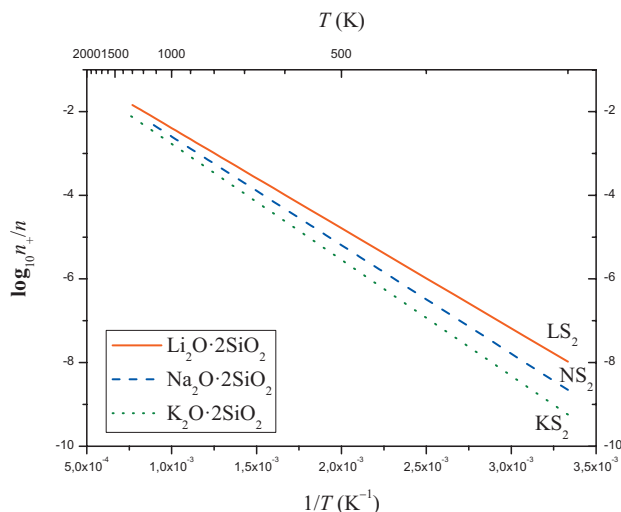


FIG. 3. Charge carrier ratios n_+/n for $\text{Li}_2\text{O}\cdot 2\text{SiO}_2$ (LS_2), $\text{Na}_2\text{O}\cdot 2\text{SiO}_2$ (NS_2), and $\text{K}_2\text{O}\cdot 2\text{SiO}_2$ (KS_2), calculated from Eq. (9). ΔH_f is taken from Table II. The marked increase of this ratio with temperature is the consequence of the activated charge carrier formation process ΔH_f , close to 1 eV.

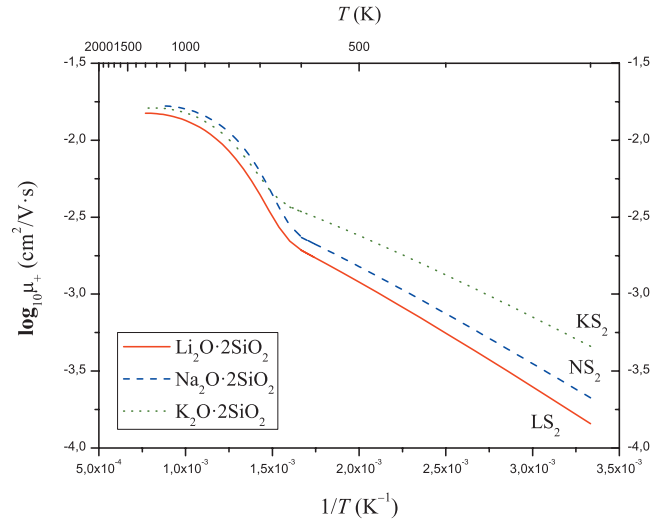


FIG. 4. Mobility μ_+ calculated from the relation $\mu_+ = \sigma/en_+$; n_+ values are taken text and results presented at Tables I and II, and σ is taken from experimental conductivity data given from Refs. 26–47.

the total concentration of the alkali cations. This fraction increases with temperature until it reaches 10^{-5} – 10^{-6} at 500 K, as presented in Fig. 3. At the same temperature, and for a glass composition ($\text{Na}_2\text{O}\cdot 0.4\text{Al}_2\text{O}_3\cdot 2.2\text{SiO}_2$) close to those we investigated here, Pitarch *et al.*⁹ also estimated a fraction of 10^{-6} of effective charge carriers from capacitance-voltage characteristics.

Finally, all these results deduced from different techniques converge towards the idea that only a very small fraction of the silver or alkali cations in glasses participate instantaneously in ionic transport. Nevertheless, the values of these fractions are only average quantities. The mobile cations at a given instant can become stationary cations at the next instant and replaced by other cations that were previously stationary. On average, the number of mobile cations remains constant. In the model we propose here, mobile cations or effective charge carriers are identified as interstitial cationic pairs that appear and disappear continuously in the glass structure. On a time scale much longer than the lifetime τ of an interstitial pair, all the cations participate in the transport process, but not all do so simultaneously. This lifetime is a function of the attempt frequency, ν , and the migration enthalpy, ΔH_m , according to

$$\tau = \frac{1}{\nu} \exp \frac{\Delta H_m}{k_B T}. \quad (16)$$

Taking $\nu = 10^{13} \text{ Hz}$ and $\Delta H_m = 0.15 \text{ eV}$, as previously calculated in Table II, an estimated value for τ at room temperature is 10^{-10} s . With a relative concentration n_+/n of about 10^{-8} at the same temperature, all the cations are expected to have moved over a distance over the mean distance between two regular sites within a time interval $\Delta t = 10^{-2} \text{ s}$. This time dependence of the number of effective moving cations has also been recently noticed by Dyre *et al.*⁵³

V. CONCLUSIONS

The results deduced from the model presented in this work are based on a microscopic description of ionic trans-

port below and above the glass transition temperature. According to the proposed model, charge carrier formation follows a temperature-activated mechanism in the entire temperature range. Mobility is also temperature-activated below the glass transition temperature but is governed by a free volume mechanism above this temperature. Fitting experimental data with the proposed expressions gives access to three fundamental parameters, i.e., ΔH_f , the enthalpy of charge carrier formation, ΔH_m , the migration enthalpy below the glass transition temperature, and the V_f^*/V_0 ratio representative of the critical free volume above the glass transition temperature.

These parameters were determined for lithium, sodium, and potassium disilicates. According to these results, charge carrier formation below T_g requires a higher energy than migration. Above T_g , charge carrier displacement requires a small free volume. For the three silicates under study, the n_+/n ratio of the number of charge carriers n_+ with the total number of alkali cations n is estimated to be 10^{-7} – 10^{-9} at room temperature, and increases up to about 10^{-2} at 1000 °C. These values are coherent with the description of glassy electrolytes as weak electrolytes. The calculated mobility at room temperature is about 10^{-4} cm² s⁻¹ V⁻¹, which is in the same order of magnitude as that measured by Hall effect in silver conducting glasses or fast ionic conductors. These values allow us to infer that the conductivity of glassy electrolytes is limited by the number of effective charge carriers rather than by their mobility.

ACKNOWLEDGMENTS

This work was financially supported by the Brazilian research funding agencies FAPESP (Process Nos. 2004/10703-0, 2007/08179-9, and 2007/03563-5), CNPq (305373/2009-9), and CAPES. J.L.S. thanks the Vitreous Materials Laboratory (LaMaV-UFSCar) for its hospitality during his contribution to this paper.

¹S. W. Martin, *J. Am. Ceram. Soc.* **74**, 1767 (1991).

²D. Ravaine and J. L. Souquet, *Phys. Chem. Glasses* **18**, 27 (1977).

³C. Kittel, *Introduction to Solid State Physics*, 7th ed. (Wiley, New York, 1996).

⁴K. Funke and R. Hackenberg, *Ber. Bunsenges. Phys. Chem* **76**, 883 (1972).

⁵C. H. J. Stuhmann, H. Kreiterling, and K. Funke, *Solid State Ionics* **154–155**, 109 (2002).

⁶V. Clement, D. Ravaine, and C. Deportes, *Solid State Ionics* **28–30**, 1572 (1988).

⁷E. Yon, W. H. Ko, and A. B. Kuper, *IEEE Trans. Electron Devices* **ED13**, 276 (1966).

⁸M. Tomozawa and D. W. Shin, *J. Non-Cryst. Solids* **241**, 140 (1998).

⁹A. Pitarch, J. Bisquert, and G. Garcia-Belmonte, *J. Non-Cryst. Solids* **324**, 196 (2003).

¹⁰E. Caillot, M. J. Duclot, J. L. Souquet, M. Levy, F. G. K. Baucke, and R. D. Werner, *Phys. Chem. Glasses* **35**, 22 (1994).

¹¹J. L. Souquet, in *Solid State Electrochemistry*, edited by P. G. Bruce (Cambridge University Press, Cambridge, 1995), p. 74.

¹²R. G. Charles, *J. Appl. Phys.* **32**, 1115 (1961).

¹³M. D. Ingram, M. A. Mackenzie, and A. V. Lesikar, *J. Non-Cryst. Solids* **38–39**, 371 (1980).

¹⁴Y. Haven and B. Verkerk, *Phys. Chem. Glasses* **6**, 38 (1965).

¹⁵J. Kawamura, R. Asayama, N. Kuwata, and O. Kamishima, in *Physics of Solid State Ionics*, edited by T. Sakuma and H. Takahashi (Research Singhpost, Kerala, India, 2006), pp. 193–246.

¹⁶M. H. Cohen and D. Turnbull, *J. Chem. Phys.* **31**, 1164 (1959).

¹⁷J. L. Souquet, M. Duclot, and M. Levy, *Solid State Ionics* **85**, 149 (1996).

¹⁸G. J. Dienes, *J. Appl. Phys.* **24**, 779 (1953).

¹⁹P. B. Macedo and T. A. Litovitz, *J. Chem. Phys.* **42**, 245 (1965).

²⁰H. Cheradame, in *IUPAC Macromolecules*, edited by H. Benoit and P. Rempp (Pergamon, Oxford, 1982), p. 251.

²¹T. Miyamoto and K. Shibayama, *J. Appl. Phys.* **44**, 5372 (1973).

²²M. Watanabe, K. Sanui, N. Ogata, T. Kobayashi, and Z. Ohtaki, *J. Appl. Phys.* **57**, 123 (1985).

²³G. Adam and J. H. Gibbs, *J. Chem. Phys.* **43**, 139 (1965).

²⁴W. Kauzmann, *Chem. Rev. (Washington, D.C.)* **43**, 219 (1948).

²⁵C. A. Angell and W. Sichina, *Ann. N. Y. Acad. Sci.* **279**, 53 (1976).

²⁶J. O' M. Bockris, J. A. Kitchener, S. Ignatowicz, and J. W. Tomlinson, *Trans. Faraday Soc.* **48**, 75 (1952).

²⁷A. E. Dale, E. F. Pegg, and J. E. Stanworth, *J. Soc. Glass Technol.* **35**, 136 (1951).

²⁸M. Hahnert, A.-R. Grimmer, and D. Kruschke, Proceedings of the 15th International Congress on Glass, Leningrad, 1989 (unpublished), Vol. 1b, p. 149.

²⁹P. L. Higby and J. E. Shelby, *J. Am. Ceram. Soc.* **67**, 445 (1984).

³⁰A. Kone, B. Barrau, J. L. Souquet, and M. Ribes, *Mater. Res. Bull.* **14**, 393 (1979).

³¹K. A. Kostanyan and E. A. Erznkyan, *Arm. Khim. Zh.* **20**, 358 (1967).

³²V. K. Leko, *Izv. Akad. Nauk SSSR, Neorg. Mater.* **3**, 1224 (1967).

³³O. V. Mazurin and E. S. Borisovskii, *Zh. Tekh. Fiz.* **27**, 275 (1957).

³⁴O. V. Mazurin and V. A. Tsekhomskii, *Izv. Vyssh. Uchebn. Zaved. Fizika* **1**, 125 (1964).

³⁵A. A. Pronkin, *Fiz. Khim. Stekla* **5**, 634 (1979).

³⁶J. L. Souquet, A. Kone, and M. Ribes, *J. Non-Cryst. Solids* **38–39**, 307 (1980).

³⁷V. I. Vakhrameev, *Steklo* **3**, 84 (1968).

³⁸M. Yoshiyagawa and M. Tomozawa, *Solid State Ionics* **23**, 271 (1987).

³⁹V. N. Boricheva, "Issledovanie elektroprovodnosti nekotorykh prostykh silikatnykh stekol v shirokom intervale temperatur," Ph.D. thesis, Leningrad, 1956.

⁴⁰K. S. Evstropiev, *Fiziko-Khimicheskie Svoistva Troinoi Sistemy Na₂O-PbO-SiO₂* (Moskva, Moscow, 1949), p. 83.

⁴¹V. V. Moiseev and V. A. Zhabrev, *Izv. Akad. Nauk SSSR, Neorg. Mater.* **5**, 934 (1969).

⁴²G. T. Petrovskii, *Silikaty* **3**, 336 (1959).

⁴³N. Shinozaki, H. Okusu, K. Mizoguchi, and Y. Suginoara, *J. Jpn Inst. Met.* **41**, 607 (1977).

⁴⁴J. L. Souquet, M. Duclot, M. Levy, *Solid State Ionics* **105**, 237 (1998).

⁴⁵S. W. Strauss, *J. Res. Natl. Bur. Stand.* **56**, 183 (1956).

⁴⁶V. G. Karpechenko, *Issledovaniya v Oblasti Khimii Silikatov i Okislov* (Moskva, Moscow, 1965), p. 84.

⁴⁷K. Hunold and R. Bruckner, *Glastech. Ber.* **53**, 149 (1980).

⁴⁸V. P. Klyuev and B. Z. Pevzner, *Phys. Chem. Glasses* **45**, 146 (2004).

⁴⁹O. V. Mazurin, M. V. Streltsina, and T. P. Shvaiko-Shvaikovskaya (Editors), *Handbook of Glass Data*, Physical Sciences Data No. 15 (Elsevier, Amsterdam, 1983), Vol. A, pp. 249–250.

⁵⁰D. S. Newman, C. Frank, R. W. Matlack, S. Twinning, and V. Krishnan, *Electrochim. Acta* **22**, 811 (1977).

⁵¹A. J. Bard and L. R. Faulkner, in *Electrochimie: Principes, Méthodes et Applications* (Masson, Paris, 1983).

⁵²W. Jost, *Diffusion in Solids, Liquids, Gases*, 3rd ed. (Academic, New York, 1960).

⁵³J. C. Dyre, P. Maass, B. Rolling, and D. L. Sidebottom, *Rep. Prog. Phys.* **72**, 046501 (2009).